

Geometry Optimization of Turbine Blade with Surface Injection

Takashi NAGUMO¹, Kazuyuki TODA² and Makoto YAMAMOTO³

¹Department of Mechanical Engineering
Tokyo University of Science

1-3 Kagurazaka, Shinjuku-ku, Tokyo, 162-8601, JAPAN

Phone: +81-3-5228-8362, Fax: +81-3-3260-4291, E-mail: nagumo@rs.kagu.tus.ac.jp

²Tokyo University of Science

³Tokyo University of Science

ABSTRACT

We have been investigating a new cycle concept for advanced propulsion system, in which hydrogen gas is directly injected from turbine blade surfaces and combusted within turbine blade passages. However, in the previous studies, we found that the aerodynamic performance of the blade is largely deteriorated due to the fuel injection. For the purpose of realizing our concept, turbine blade is required to have the adequate performance even with the hydrogen injection. In the present study, we develop a geometry optimization procedure for turbine blade with air injection. Our procedure is based on the gradient method, and composed of some elements, including CFD, geometry modification and automatic design point arrangement, in which design points are automatically clustered around the complicated surface. The validity of our approach is demonstrated by applying the geometry optimization to 2 types of turbine blades with different injection patterns.

INTRODUCTION

Recently, a lot of environmental issues such as air pollution and global greenhouse effect are focused on, which are mainly caused from NO_x, SO_x and CO₂ exhausted by combustion. On the other hand, with the advancement of engineering technologies, the requirements of gas turbine have become more severe. The propulsion system for next generation aircraft needs to have higher power, lighter weight and lower emissions than existing ones. In terms of thermodynamics, hydrogen gas is the best fuel, because it has some effectual features such as high energy per unit weight, high reaction rate and wide range of flammability. Furthermore, hydrogen is a very clean fuel, as it does not produce SO_x and CO₂ in the exhausted gas. Therefore, hydrogen is expected to be an alternative energy against conventional fossil energy resources, and to be a promising one for many applications in the near future.

Considering these backgrounds, we have proposed a new cycle concept for hydrogen-fuelled aircraft propulsion system (Nagumo et al., 2000). Our concept is that the combustion process is not handled within combustion chamber, but within turbine stages, namely, the concept will enable us to realize the combustor-less aircraft engine. We have been investigating the concept by means of cycle analysis and numerical simulations. In the previous study, carrying out the thermodynamic cycle analysis with the assumption that the chemical reactions of hydrogen combustion come to be equilibrated within each turbine stage, we demonstrated that the engine performance with our cycle have many advantages as compared with that with conventional GE90

engine cycle (Nagumo et al., 2001). Moreover, in order to investigate the combustion phenomena within turbine blade passage, we performed numerical simulations for the turbulent flow field with hydrogen-fuelled combustion, in which hydrogen gas was directly injected from turbine blade surface and combusted within turbine blade passage. From the computational results, we confirmed that the hydrogen reacts with air sufficiently in a turbine blade passage because of the high reaction rate of hydrogen combustion (Nagumo et al., 2001). However, we also found the shortcoming of our system, which is that the adequate expansion of the burnt gas cannot be achieved within the turbine stage, since the aerodynamic performance of the blade is largely decreased due to fuel injection. This is caused from the fact that the turbine blade applied in the previous study has been already designed to optimize the performance at the case without fuel injection. Therefore, for the purpose of realizing our concept, we have to develop the design method, in which the optimal performance has been accomplished at the case with hydrogen injection.

The development of computational technology has been playing an important role in turbomachinery blade design. The use of computational fluid dynamics (CFD) has been achieved considerable reduction in the design time. In many cases, however, the blade design still depends on the empiricism by a number of modifications of the blade geometry and verifications through wind tunnel tests or numerical calculations. Such a design process can be very time consuming, and may result in a high design cost. Therefore, many researches are currently reported, aiming at the conversion of the design process based on trial and error into automatic one by applying an optimization algorithm to the turbomachinery blade design (Goto et al., 1999). Optimization design is defined as the problem to determine an optimal solution by means of forward analyses and perturbations with respect to design variables in the design space, which minimizes the objective function that represents desired requirements with satisfying a set of constraints. In most of fluid dynamics optimization problems, CFD is generally employed as the forward analysis procedure. Since a large number of calculations have to be needed during optimization process, the computational load for optimization procedure becomes significantly high even with existing high-performance computers. Thus, it is expected the development of more efficient optimization algorithm which reduces the number of forward analyses for the decision of optimal solution. On the other hand, most of the applications of optimization procedure to turbomachinery designs are the blade geometry optimizations of cascade aimed at the improvement of aerodynamic performance, and are not reported for more complicated object that needs larger flexibility.

In the present study, we focus on the geometry optimization of

Since the optimization in this study aims at the design of turbine blade with air injection, it is expected that the blade geometry changes largely around the air injection slot. Therefore, in order to enable the geometry modification with large flexibility by the minimum design variables, the mechanism of automatic design point arrangement, in which design points are automatically clustered around the complicated surface or eliminated from the uncomplicated one, is introduced in our procedure.

Fig. 2 illustrates the initial shape of turbine blade and the design points employed in this study. In order to construct the blade geometry, several parameters of chord length, pitch length, stagger angle and radius of trailing edge are fixed as design conditions. The design variables are defined for the representation of camber line and turbine blade surface as follows:

The locations of leading and trailing edges being fixed at $(x_c, y_c)_{LE} = (0,0)$ and $(x_c, y_c)_{TE} = (1, \bar{y}_c)$, and the camber line being defined as a cubic function, a typical camber line has been formulated in the next equation,

$$y_c = ax^3 + (\bar{y}_c - a)x^2, \quad x \in [0,1] \quad (4)$$

where the coefficient a is chosen as one of the design variables \bar{D} . The whole blade geometry is modified by the perturbation of this variable.

Turbine blade geometry is represented by a cubic B-spline curve passing through the leading and trailing edges in this study. The advantage of cubic B-spline representation is the 2nd order of continuity inherent in the cubic B-spline curve. This high order of continuity allows parameters to be varied with the ability to generate a great variety of physically realistic blade shapes. Several control points that can be changed to modify the blade geometry are arranged around the blade surface. These control points are used as the design points during the optimization process. The perpendicular distance from each design point to camber line is defined as an element of the design variables \bar{D} .

Here, we note the geometrical constraints of design points imposed for the construction of blade geometry. The leading edge (corresponding to the leading point of camber line) and the radius of trailing edge are fixed during the optimization process. Furthermore, since the blade must have a finite thickness, the design points defining the pressure and suction surfaces cannot be crossed to each other.

Nonlinear Optimization Algorithm

The present nonlinear optimization problem is solved employing the gradient method, which is well known as a basic optimization strategy. In the gradient method, the following defects are mentioned. Since the search space depend on an initial set of design points, the solution may fall into a local optimum. The turbine design problem is multimodal, and consequently, there is no guarantee, which can always accomplish the global optimum. The objective of our design is to search the optimal geometry that exists in the nearest original turbine blade. Hence, it is not necessary to consider the above theoretical problem of the gradient method.

In our procedure, the optimal solution with respect to each design variable is calculated one by one according to the design sequence described in the previous section. The process starts with an initial set of design variables. The design is then updated using an iterative procedure given by

$$d_i^{k+1} = d_i^k + \alpha^k p^k \quad (5)$$

where the superscript k is the iteration number, and the subscript i denotes the i -th element of design variables \bar{D} . The vector p is the search direction, and the scalar α is the step size to move in the direction p . In case of the design for camber line, because the parameter a described in Eq. (4) is a scalar value, the search direction p is set to 1. In the other cases, the search direction p is set with the unit vector arising from the design point in the direction

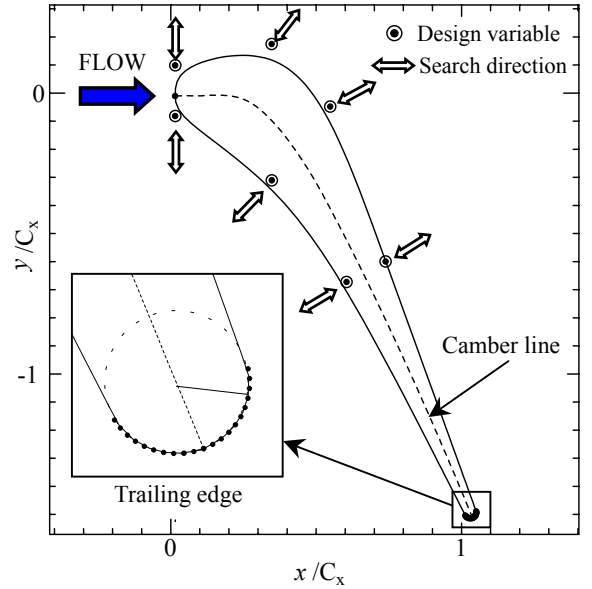


Fig. 2 Design variable and blade shape for initial design

normal to the camber line. As the result, Eq. (5) is reduced to the next one-dimensional optimization problem.

$$\min F(d_i^k + \alpha^k p^k) = \min F(d_i^k + \alpha p^k) \quad (6)$$

We solve the above one-dimensional problem by employing the modified Davies, Swann and Campey method (Box et al., 1969). The detailed description of the method and the modification are given in the following part.

At first, the optimization process starts with an initial guess of the step size and search direction. The procedure calculates the objective function by shifting one of the design variables along the search direction. Here, the gradient of objective function with respect to each design variable is estimated by using a finite difference method. For example, the i -th element of design variables \bar{D} is defined by next equation.

$$\frac{\partial F}{\partial d_i} = \frac{F(d_i + \alpha p) - F(d_i)}{\alpha} \quad (7)$$

Based on the information of the gradient, the search is iterated in the direction where the objective function decreases, and the next search point is evaluated. On the other hand, if the objective function increases in the first evaluation, the search direction is changed in reverse. These processes are continued until the objective function increases from the last value. In this step, it has been accomplished the state where the minimum point exists in the search space. Assuming the objective function to be a quadratic function, the algorithm calculates the parameter a given the local minimum by implementation of parabolic interpolation using the last three design variables. After carrying out forward analysis once again in the obtained parameter a , the local minimum has been determined by comparing the function value among the last four design variables. Since the solution obtained by this procedure depends on the step size guessed at initial design conditions, the above procedure is performed at two times, which the step size is changed into the smaller one.

Automatic Design Point Arrangement

In the gradient method, the sufficient solution may not be obtained depending on the initial definition of design points. Moreover, the design objective in this study is considered as a complex geometry, so it is difficult at initial design to put the design points in the area where large geometry modification will be

expected. Therefore, the mechanism of automatic design point arrangement, in which design points are automatically clustered around the complicated surface, is introduced into the present optimization procedure.

It is defined as one optimization step that all the design variables $\vec{D} = (d_1, d_2, \dots, d_n)$ are modified at one time. If the change rate of objective function is 10 % or less as compared with that of the previous step after one optimization step completed, the generation of design point is performed in order to improve the flexibility of geometry modification. The generating location of new design point is determined due to searching the blade surface, where it is suspected the number of design points to be insufficient for the further improvement. Our procedure search the maximum area of the difference of pressure coefficient defined with an adjacent design points, and put a new design point in the center between the adjacent ones. In addition, when a new design point is generated, all the design variables are corrected so that the blade shape obtained in this process can be maintained.

On the other hand, if the pressure distributions around a certain design point are sufficiently close to the required ones, the modification for the design point reduces the efficiency of the overall optimization. In this process, if the pressure distributions are converged at the required one, and the removal of the design point are not influenced on the change of blade area, which is 0.1 % or less as compared with that of the previous step, the corresponding design point is eliminated.

CFD PROCEDURE

Governing Equations

In the optimization problem, the governing equations mean the equality constraints $C_j = 0$ described in Eq. (1). As the design target of this study is a turbine cascade, the flow field is assumed to be two-dimensional turbulent flow. In addition, time averaged variables are dealt with. Therefore, the Reynolds-averaged compressible continuity, Navier-Stokes and total energy equations are employed as the governing equations. These equations are written as follows:

$$\frac{\partial \bar{\rho}}{\partial t} + \frac{\partial}{\partial x_k} (\bar{\rho} \tilde{u}_k) = 0 \quad (8)$$

$$\frac{\partial \bar{\rho} \tilde{u}_i}{\partial t} + \frac{\partial}{\partial x_k} (\bar{\rho} \tilde{u}_i \tilde{u}_k + \bar{p} \delta_{ik}) = \frac{\partial}{\partial x_k} (\bar{\tau}_{ik} - \bar{\rho} u_i'' u_k'') \quad (9)$$

$$\frac{\partial \bar{\rho} \tilde{e}}{\partial t} + \frac{\partial}{\partial x_k} \{ \tilde{u}_k (\bar{\rho} \tilde{e} + \bar{p}) \} = \frac{\partial}{\partial x_k} (\bar{\tau}_{ik} \tilde{u}_i - \bar{q}_j) \quad (10)$$

Taking the Boussinesq's hypothesis, Reynolds stress tensors are expressed in the next form,

$$-\bar{\rho} u_i'' u_k'' = \mu_t \left(\frac{\partial \tilde{u}_i}{\partial x_k} + \frac{\partial \tilde{u}_k}{\partial x_i} - \frac{2}{3} \frac{\partial \tilde{u}_l}{\partial x_l} \delta_{ik} \right) - \frac{2}{3} \bar{\rho} k \delta_{ik} \quad (11)$$

where turbulent viscosity coefficient μ_t is obtained by employing the high-Reynolds-number type $k-\varepsilon$ model (Launder and Spalding, 1974).

Numerical Procedures

In the present study, the governing equations are discretized by using a finite difference method. 2-stage Runge-Kutta method is employed to the time integrations. And, considering the numerical stability and accuracy, we apply 2nd-order upwind TVD scheme (Yee and Harten, 1987) to the inviscid terms, and 2nd-order central differencing scheme to the viscous ones. Furthermore, the efficiency of the computations is increased by the local time marching technique.

CFD occupies most of the computational load during the optimization, so it is contributed directly to the improvement of the whole optimization efficiency to achieve the efficient convergence

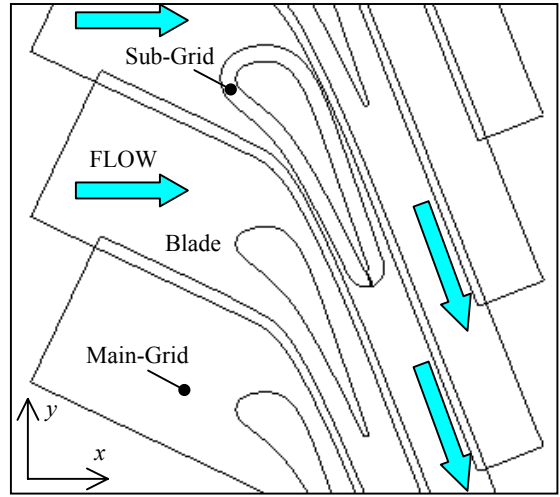


Fig. 3 Grid arrangement of turbine blade cascade

of the flow field. Considering that the influence of blade modification on the flow field is small, the solutions obtained in the previous analysis are used for the initial CFD conditions. This treatment reduces the computational load drastically.

Computational Grid

The grid modification is repeated with the change of blade geometry during the optimization. In this study, we employ the overlapping grid method in order to simplify the automatic grid generation. The computational grids are arranged as shown in Fig. 3. The grids consist of 2 components, which are main-grid laid over the flow field within a turbine blade passage and sub-grid fitted to the turbine blade surface. Only sub-grid is remeshed with fitting to the blade geometry during the design process. The calculations for the flow field within the turbine blade passage and in the vicinity of the blade are carried out with the main-grid and sub-grid, respectively. The transport variables in the overlapped space have to maintain the consistency between each grid. The variables in the overlapped region are interpolated linearly with variables on the other grid. The grid points are arranged at 72×44 for main-grid and 127×21 for sub-grid. A certain amount of grid points are clustered near the blade surface.

Boundary Conditions

The boundary conditions are imposed as follows: At inflow boundary in the main-grid, total pressure, total temperature and incident angle are fixed and Mach number is extrapolated from the computational region. At outflow boundary, static pressure is fixed and other variables are extrapolated from inside. At periodic boundary in the main-grid and branch cut in the sub-grid, all variables are set equal. On the blade surface, no-slip and adiabatic conditions are imposed, and the general wall function is employed. At the air injection slot, static pressure is extrapolated from the inside and other variables are fixed by injecting conditions. As mentioned above, the variables for the overlapped boundary are interpolated linearly from the variables on the other grid.

Computational Conditions

Fig. 2 illustrates the schematic figure of the linear turbine cascade employed in this study. The chord length is 51.55 mm, the pitch length is 36.0 mm, the incident angle is 0 deg., and the stagger angle is 56.0 deg. The first turbine stator is dealt with as our design object. In our cycle concept, air passed through a compressor flows into turbine stage directly, so the turbine inflow conditions are determined as that of combustion chamber inlet derived from cycle analysis. These geometries and computational conditions are summarized in Table 1.

Table 1 Turbine parameters

Chord length	[mm]	51.55
Pitch length	[mm]	36.0
Stagger angle	[deg.]	56.0
Incident angle	[deg.]	0.0
Inflow total temperature	[K]	903.4
Inflow total pressure	[MPa]	3.92
Outflow static pressure	[MPa]	3.36

The design points for the initial turbine blade are defined as follows: Several control points, which construct a closed cubic B-spline curve, are arranged as shown in Fig. 2. These points consist of 3 points near the blade pressure side, 4 points near the suction side, 1 point at the leading edge and 20 points around the trailing edge. Among these points, 7 points near the suction and pressure sides are selected as the design points. Including the parameter a for the construction of camber line, the total design variables become 8 parameters at an initial design condition. In addition, the control points for trailing edge can be changed depending on the camber line due to geometrical constraint, with keeping the radius of trailing edge constant.

Injecting Conditions

In our concept, hydrogen gas is injected from turbine blade surface into the blade passage. However, in this paper, considering the computational load for the flow field with hydrogen combustion, we handle air as the jet medium in order to reduce the additional load. The injecting conditions of air are based on that with hydrogen gas.

The following injecting conditions are applied. In the case of slot injection, the injector, which the width is 3.0 mm, is installed on the blade suction side at the location of $x/C_x = 0.3$. Here, C_x means x component of the blade chord length. Although the blade geometry changes during the optimization process, the jet location with respect to x direction is always fixed. In addition, the injecting velocity is fixed at 150 m/s, which corresponds to the 10% in volume for the inflow air. On the other hand, the case of all injection means that air is injected from all blade surfaces, which models the injection with using turbine blade made by porous media. The injecting velocity is determined by the conditions that the amount in volume is equal to that of slot injection. In both cases, the static temperature of air is 900 K, and the injecting direction is 30 deg. to the blade surface.

RESULTS AND DISCUSSIONS

Application for Slot Injection

The following results are obtained at 20 optimization steps and the design variables are increased to 12 including the camber line. Fig. 4 indicates the comparison of surface pressure coefficient for initial and optimal geometries. The vertical and horizontal axes denote the pressure coefficient and the location of x direction normalized with C_x , respectively. In the figure, black symbols, broken line and solid one correspond to the performance without surface injection, namely, the original performance of turbine blade employed in this study, and that with surface injection for initial and optimal geometries, respectively. It has been apparent that the aerodynamic performance is much decreased due to injecting air from the blade surface, and the conventional performance cannot be accomplished with the initial blade. As can be seen in the figure, the pressure coefficient distributions are improved considerably in all regions except the location of $x/C_x = 0.6$ on the blade suction surface. Since the objective function is set up with the surface pressure coefficient in the present optimization, we can consider that our procedure works for the turbine blade geometry optimization effectively.

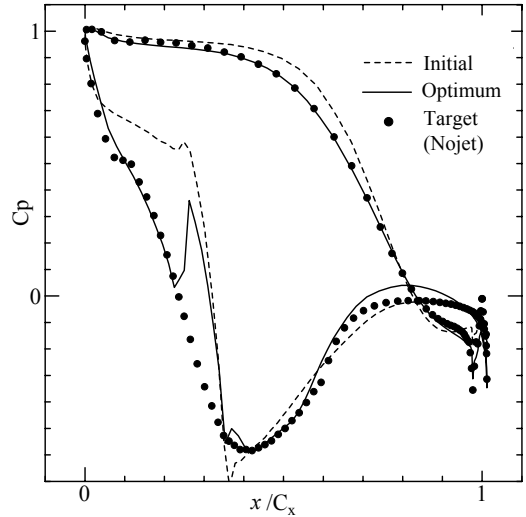


Fig. 4 Comparison of pressure distributions on the blade for initial and optimized designs

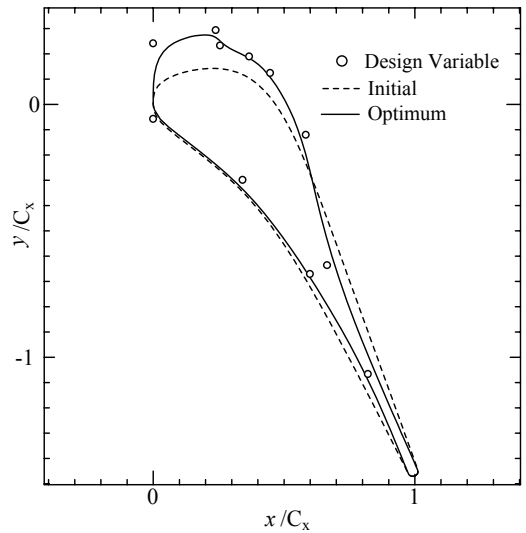


Fig. 5 Variation of blade geometry for initial and optimized designs

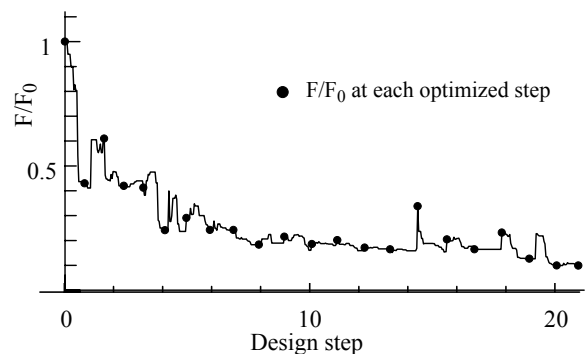


Fig. 6 Convergence history of normalized objective function

Fig. 5 shows the variation of blade geometry for initial and optimal designs. In the figure, the vertical and horizontal axes are the coordinate normalized with C_x . The large geometry modification is observed around the air injection slot in the optimal blade. Moreover, as shown in Fig. 2, although the design points were arranged almost the same distance as each variable near the blade suction and pressure sides in the initial design, these points have

been clustered near the air injection slot on the blade suction surface. Because the design points are distributed locally, the large change can be expressed, and it is thought that the complicated pressure coefficient distributions near the slot are also improved to the design target.

Fig. 6 provides the convergence history of the objective function, where the function value is estimated all over the blade surface except for that on the injection slot. The vertical and horizontal axes denote the objective function normalized with that of initial design and design step which means the number of iteration. From this figure, we can see that the objective function is decreased by 90 % as compared with that of initial design at 20 optimization steps. We can also understand that the convergence to insufficient solutions of the objective function is avoided due to the automatic design point arrangement introduced in our procedure.

Application for All Injection

The results for the all injection case are discussed in the following section, which are obtained at 7 optimization steps and the design variables are increased to 12. Fig. 7 and Fig. 8 denote the comparisons of surface pressure coefficient distributions and the blade geometry for the initial and optimal designs, respectively. As mentioned in the slot injection case, the results are written with broken and solid lines corresponding to that of initial and optimal blade geometries. As can be seen in Fig. 7, the local changes of surface pressure coefficient (i.e. spike), which have been seen in the slot injection, are not observed in this case. However, the surface pressure on the blade suction side is considerably high as compared with the target performance. This is because the flow structure corresponds to that around the thicker blade, due to the injection from all the blade surfaces. As shown in Fig. 7, also in this case, the pressure coefficient distributions of the optimal geometry are in good agreement with the required performance on both suction and pressure sides. Therefore, it is clear that our procedure is appropriate for the blade geometry optimization. Moreover, from Fig. 8, we can understand that the blade thickness around the rear part of suction side becomes thin in the optimal geometry. Fig. 9 shows the objective function versus the design iteration. It should be noted that the objective function is estimated all over the blade surface. It is accomplished at 7 optimization steps that the objective function has been improved by the required performance about 85% as compared with that of initial design.

Overall Discussion

Through the computational results for both cases, the validity of our approach has been demonstrated to geometry optimization of turbine blade with surface injection. The blade geometry obtained with the present optimization increased the thickness around the leading edge. Due to this modification, the surface pressure was decreased to the required performance by accelerating the flow around the turbine blade. We can consider that such geometry modification has the consistency with that expected from the required performance.

On the other hand, the optimal blade geometry obtained with our optimization has the common tendency, which as for the suction side, the blade thickness increases in the front part and it becomes very thin in the rear part. This is caused from the following reasons. One reason is that the optimization is performed for each design variable according to the constant design sequence, so the optimal solution may depend on the sequence. The further investigations are needed for the procedure in terms of the influence of the design sequence on the optimal solution. The other reason is that since the present optimization uses the objective function defined in Eq. (2), it may be taken only the pressure coefficient distributions in x direction into consideration in the design process. Due to this formulization, the influence of the blade modification around the leading edge on the objective function is too small. Therefore, although the effect of surface pressure

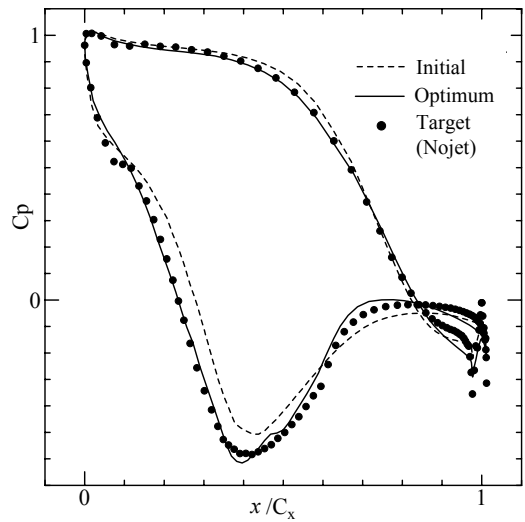


Fig. 7 Comparison of pressure distributions on the blade for initial and optimized designs

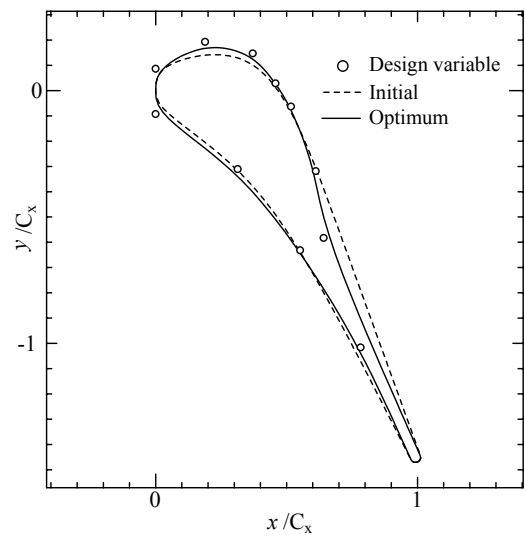


Fig. 8 Variation of blade geometry for initial and optimized designs

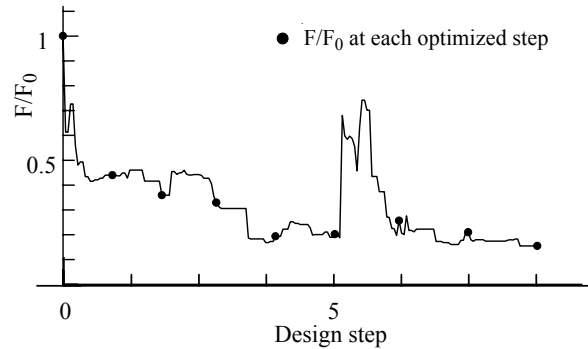


Fig. 9 Convergence history of normalized objective function

distributions on the lift is reflected correctly, it is not affected the effect on the drag to the optimal solution. The further investigations are required for the formulation of objective function.

CONCLUSION REMARKS

In the present study, we focused on the geometry optimization of turbine blade with surface injection. Integrating the forward analysis based on CFD with a nonlinear optimization algorithm, we

developed the optimization procedure for the design of turbine blade. In addition, the validity of our approach was demonstrated by applying the geometry optimization to 2 types of turbine blades with different injections. This study can be summarized as follows:

1. The present procedure is appropriate for the blade geometry optimization. It is accomplished that the objective function has been improved by the required performance about 90% as compared with that of initial design.
2. Due to the modification that increases the blade thickness around the leading edge, the surface pressure was decreased to the required performance by accelerating the flow around the turbine blade. It can be considered that such geometry modification has the consistency with that expected from the required performance.
3. If only the effect of surface pressure distributions on the lift is considered, it can be said that the blade geometry obtained with the present procedure has the same aerodynamic performance with and without surface injections.
4. The automatic design point arrangement enabled the convergence to sufficient optimal solution, and the flexible response to the local change of blade geometry by the minimum design variables.

REFERENCES

- Nagumo, T., Toda, K. and Yamamoto, M., 2001, "Cycle Analysis of Hydrogen-Fuelled Combustion within Turbine Blade Passage", *Proceedings, 6th International Conference on Technologies and Combustion for a Clean Environment*, Vol.1, pp.73-79.
- Nagumo, T., Toda, K. and Yamamoto, M., 2001, "Numerical Investigations of Hydrogen-Fuelled Combustion within Turbine Blade Passage", *JSME Journal*, 67-659, B, pp.1672-1679.
- Goto, A., Ashikawa, K., Sakurai, T. and Saito, S., 1999, "Compact Design of Diffuser Pump Using Three-Dimensional Inverse Design Method", *ASME Fluids Engineering Division Summer Meeting*, FEDSM99-6847, pp.1-14.
- Kodama, Y. and Hino, T., 1999, "Effect of Body Geometry Expression and Grid Resolution on the Optimization of a Two-Dimensional Symmetric Wing", *Proceedings ASME/ASME Joint Fluids Engineering Conference*, pp.1-6.
- Box, M. J., Davies, D. and Swann, W. H., 1969, "Nonlinear Optimization Techniques", ICI Ltd., Monograph No.5, Oliver and Boyd, Ltd.
- Lauder, B. E. and Spalding, D. B., 1974, "The Numerical Computation of Turbulent Flows", *Comput. Meth. Appl. Mech. Eng.*, 3, pp.269-289.
- Yee, H. C. and Harten, A., 1987, "Implicit TVD Schemes for Hyperbolic Conservation Laws in Curvilinear Coordinates", *AIAA Journal*, 3, pp.266-274.